DESIGN OPTIMIZATION OF NATURAL LAMINAR FLOW FUSELAGES IN COMPRESSIBLE FLOW

Simha S. Dodbele*
ViGYAN, Inc., Hampton, VA

ABSTRACT

A computational method has been developed to design axisymmetric body shapes such as fuselages, nacelles and external fuel tanks with increased transition Reynolds numbers in subsonic compressible flow. The new design method involves a constraint minimization procedure coupled with analysis of the inviscid and viscous flow regions, and compressible stability analysis of the boundary-layer. Boundary-layer transition is predicted by a "hybrid" transition criterion based on Granville's transition criterion and a criterion using linear stability theory coupled with the e^n-method. The method can be used to design body shapes for a specific n-factor chosen to suit a particular application. A tiptank of a business-jet is used as an example to illustrate that the method can be used to design an axisymmetric body shape with extensive natural laminar flow. Boundary layer transition is predicted to occur at a transition Reynolds number of 6.04×10^6 on the original tiptank. On the designed body shape a transition Reynolds number of 7.22×10^6 is predicted.

NOMENCLATURE

A/A_0	Ratio of local disturbance amplitude to amplitude at the point of neutral stability for a fixed disturbance frequency
C_D	Body drag coefficient (based on frontal area)
$C_p(x)$	Pressure coefficient
D	Maximum diamter, ft
f_r	Fineness ratio (body length/maximum body diameter)
f_{obj}	Objective function
L	Body length, ft
M	Freestream Mach number
NLF	Natural laminar flow
n	Logarithmic exponent of amplitude-growth ratio of unstable Tollmien-Schlichting wave, $n = \ell n(A/A_0)$
n_f	Total number of design variables representing body radii in the forebody region
n_a	Total number of design variables representing body radii in the aftbody region
R_L	Reynolds number based on freestream conditions and body length
R´	Unit Reynolds number based on freestream conditions
r_{f_i}	Body radius at x_{f_i} in the forebody region, ft
r_{Lf_i}	Lower bound for the body radius r_{f_i} in the forebody region, ft
r_{Uf_i}	Upper bound for the body radius r_{f_i} in the forebody region, ft
r_{a_i}	Body radius at x_{a_i} in the aftbody region, ft
r_{La_i}	Lower bound for the body radius r_{a_i} in the aftbody region, ft
r_{Ua_i}	Upper bound for the body radius r_{a_i} in the aftbody region, ft
T-S	Tollmien-Schlichting
T(y)	Boundary-layer temperature profile, R
U(y)	Boundary-layer velocity profile, ft/sec
V	Volume of the body, cu ft
X	Axial coordinate starting at nose, ft
X_m	Axial coordinate of the maximum thickness point, ft
X_{tr}	Axial coordinate of transition starting at nose, ft
x	Nondimensional axial coordinate, X/L
x_{tr}	Nondimensional axial coordinate of transition, X_{tr}/L
$x_{tr}(g)$	Nondimensional transition location by Granville's criterion
$x_{tr}(e^n)$	Nondimensional transition location by e^n-method
$x_{tr}(h)$	Nondimensional transition location by the hybrid transition criterion
ψ	Obliqueness of T-S disturbances with respect to streamlines, deg
2-D	Two-dimensional flow

Subscripts

tr	Transition
f	Forebody
a	Aftbody
i	i-th point

* Research Scientist

L Lower bound
U Upper bound

INTRODUCTION

Recent advancement in airplane construction techniques and materials employing bonded and milled aluminum skins and composite materials allow for the production of aerodynamic surfaces without significant waviness and roughness, permitting long runs of natural laminar flow (NLF) over wings in subsonic flow. These advances lead to excellent opportunities for airplane drag reduction by increasing the extent of NLF over wings [1]. In the last decade, computational and experimental laminar-flow and drag reduction programs have reached a level of maturity as far as the lifting surfaces are concerned. But laminar flow research on nonlifting airframe surfaces, such as fuselages, nacelles, and external fuel tanks, has received limited attention [2,3]. Previous investigations [4-6], conducted mainly at incompressible speeds, indicate that with proper body shaping a potential exists for achieving substantial runs of laminar flow over axisymmetric bodies with transition Reynolds numbers as high as about 20 million [4].

In high subsonic flows, compressibility has a favorable effect on laminar boundary layer stability. The application of NLF technology to high speed, subsonic fuselages could take advantage of this favorable influence of compressibility on the stability of two-dimensional and axisymmetric boundary layers [7].

In refs. [2] and [3] a computational design procedure was developed to obtain fuselage shapes with increased extent of laminar flow and reduced drag coefficients at incompressible speeds. An optimization procedure was coupled with an aerodynamic analysis program which predicted transition location using Granville's criterion. It was indicated that a transition-prediction criterion based on linear boundary-layer stability theory coupled with the e^n method (originally introduced by Van Ingen [8] and Smith [9]) appears to be a more reliable approach to predict onset of transition in the design of NLF fuselages [10-13]. However, since the prediction of onset of transition using linear stability analysis coupled with the e^n-method (from here onwards referred to as the e^n-method for brevity) alone in the design procedure will be very expensive, a "hybrid" transition criterion based on Granville's transition criterion and a transition criterion based on the e^n-method may be more practical in the design calculations.

This paper presents a new design method in which a hybrid transition criterion based on the Granville's transition criterion and the e^n-method has been incorporated to generate body shapes with increased transition Reynolds numbers at subsonic compressible speeds. Design calculations for a tiptank in compressible flow are presented as an example case.

BACKGROUND

References 4-6 published results of mostly incompressible under-water transition experiments on bodies of revolution with varying fineness ratio, indicating maximum transition-Reynolds numbers of about 20 million for low fineness ratio bodies. Reference 3 presents a recent overview of incompressible transition experiments on axisymmetric bodies. The extent of laminar flow in incompressible flow is influenced and constrained by the steepness of the surface pressure gradients in the axial direction and the magnitude of the minimum surface pressure, both of which are related to the fineness ratio of the axisymmetric body [14].

The transition process over an axisymmetric body shape at zero angle of attack is caused by large-amplitude growth of Tollmien-Schlichting (T-S) disturbance waves in the laminar boundary-layer flow. In compressible flow, the presence of the density gradients in the boundary layer in the direction normal to the wall in addition to the velocity gradients can result in a large reduction in the spatial growth of T-S disturbances in the laminar boundary layer.

A recent study [7] of bodies of revolution at high, subsonic speeds without supersonic regions (subcritical flow) demonstrated the potential for tripling the length of sufficiently stable laminar flow at $M = 0.8$ and $R_L = 40 \times 10^6$, in comparison with incompressible speed at the same length Reynolds number. A benchmark wind-tunnel transition experiment was conducted in the NASA-Ames 12-ft. pressure tunnel in the 1950's by Boltz et al., [15, 16] at high subsonic freestream Mach numbers, measuring the transition locations on two ellipsoids of fineness ratios (f_r) of 7.5 and 9.14. Transition occurred as far downsteam as 80 to 88% for M = 0.90 to 0.96, due to a favorable combination of flow acceleration, Mach number, Reynolds number and weak acoustic environment in the tunnel. Reference 17 presents correlation of compressible boundary-layer-stability analysis done for several of the experimental results reported by Boltz et al., and indicates that integrated T-S linear logarithmic amplification factors (n-factors) of 8-11 are obtained at the point of measured transition onset. As a result of the increase in the laminar flow at compressible flow conditions, the total drag was reduced by more than 50 percent as the Mach number approached 0.95.

The favorable damping effect of the T-S waves in compressible flow contributes to the achievement of increased transition-Reynolds numbers on lifting as well as nonlifting aircraft surfaces in the absence of strong crossflow [7]. This favorable effect of compressibility should be exploited in the design of advanced NLF bodies for application to general aviation, commuter, transport and business aircraft.

To date, no optimization study has been performed to help understand the design of axisymmetric, laminar-flow body shapes for high-speed applications utilizing the increased stability of the laminar boundary layer at compressible flow conditions. Computational drag minimization studies have been conducted for incompressible flow problems by Dalton and Zedan [18], Parsons, et al. [19], Pinebrook and Dalton [20] and Wolfe and Oberkampf [21]. Some of the preceding studies used axial singularities, thus restricting design applications to only a limited class of body shapes. Smith, et al. [22] undertook design of

axisymmetric bodies by shaping the aft-portion to minimize turbulent drag over the aftbody and flow separation near the tail.

Reference 2 presented a numerical optimization method to design axisymmetric aircraft fuselage shapes under incompressible flow conditions. An optimization procedure was coupled with an aerodynamic analysis program which predicted transition location using Granville's criterion based on integral boundary-layer methods. It was found that the Granville's transition criterion had limitations for predicting transition on axisymmetric bodies of fineness ratios of 6-10 (of interest for aircraft fuselages). The analysis also indicated that a consistent transition-prediction method based on the e^n-method provides a more realistic transition criterion for use in design calculations.

OPTIMIZATION PROCEDURE FOR NLF BODY DESIGN

The design method developed to obtain body shapes with extensive runs of laminar flow is illustrated in the flowchart (Fig. 1). There are several methods available for optimization in engineering applications, e.g., constrained minimization [23], quasi-Newton [24], and evolution methods [25]. The constrained minimization method developed by Vanderplaats, (CONMIN) [23], has been used in the present investigation. The constrained minimization method is coupled with analysis of the inviscid and viscous flow regions, linear stability analysis of the compressible boundary-layer and a transition prediction method.

Initial values of the design variables describing the body shape are input along with the length Reynolds number, Mach number of the free stream, and the fineness ratio of the desired body shape. The axisymmetric body is described by design variables r_{f_i} $(i=1,n_f)$ and r_{a_i} $(i=1, n_a)$ representing the body ordinates at the axial locations x_{f_i} $(i=1,n_f)$ in the forebody section and x_{a_i} $(i=1,n_a)$ in the afterbody section (see Fig. 2). By having a large number of design variables in the forebody region, the forebody can be represented in great detail especially near the nose region [14]; and such detailed representation can incorporate small body perturbations dictated by the design cycles. Tollmien-Schlichting -dominated laminar flow depends on the local pressure gradient, which is determined by the local curvature of the surface. For a given minimum surface pressure level, an increased extent of laminar flow can, in principle, be obtained by properly designing local pressure gradients along the body through body surface perturbations. Such detailed shape representation contributed to the design of advanced two- dimensional (2-D) NLF airfoils [26].

The aerodynamic analysis program used in the present optimization procedure is based on a low-order, surface-singularity method (VSAERO) [27]. Both pressure and velocity distributions can be computed by this method which uses surface singularity panels to represent the body shape. The Karman-Tsien compressibility correction is incorporated in the surface-panel method to predict aerodynamic properties accurately in high-subsonic subcritical flow conditions. Still, the surface-panel methods with compressibility corrections cannot properly model the inviscid flow around the body if the flow field has embedded supersonic flow regions. The example body shape considered in the present investigations did not have any supersonic regions in the flow field. A modified version of a finite-difference, full potential/Euler method (RAXBOD) [28] can be incorporated in the program if the flow field has mixed subsonic-supersonic zones.

The boundary-layer profiles along the surface of the body, required for e^n-method, are generated by a modified axisymmetric boundary layer code (HARRIS) [29]. The program can handle adiabatic, nonadiabatic, injection or suction wall conditions. The boundary layer program calculates detailed boundary-layer velocity and temperature profiles along with their first and second derivatives normal to the surface, including the effects of transverse curvature.

Laminar boundary-layer stability analysis along the body is done by using compressible linear stability theory. The COSAL program [30] solves the finite-differenced, boundary-layer stability equations by using matrix methods. The compressible T-S eigenvalue problem is solved for each boundary-layer station along the body surface giving temporal growth rates of the instability waves propagating at specific wavelengths and wave angles. The temporal growth rates are transformed to the spatial growth rates using Gaster's phase-velocity relationship [31]. Boundary-layer transition is predicted by the e^n-method in which n, usually referred to as n-factor, is obtained by integrating the linear growth rate of the T-S waves from the neutral stability point to a downstream location on the body.

The correlation of a large number of wind tunnel data and flight transition experiments with linear boundary-layer stability calculations has made the e^n-method a reliable transition-prediction method (see [12]). For experiments in wind tunnels with low turbulence and low acoustic levels the onset of transition can be correlated with an n-factor of 9 to 11 in subsonic, transonic and supersonic flows. In the case of flight tests, higher n-factors of the order of 12 to 15 have been observed to correlate transition. In the present design calculations, the n-factor in the design method can be chosen so as to suit a particular application- e.g., to design a body for a wind tunnel, a flight test article, or an underwater body.

In the present method a "hybrid" criterion based on Granville's transition criterion and the e^n-method transition criterion is used for predicting boundary-layer transition. In the hybrid transition method, Granville's criterion is used to calculate gradients of the objective function; average value of the transition locations predicted by applying Granville's criterion and the e^n-method criterion is used for predicting transition for use in the functional value at the end of each iteration in the design. Though the method has the capability of designing a body shape by the e^n-method alone, it is found that such a calculation will take large amount of computer time. For this reason the hybrid criterion is formulated for predicting transition

in the design calculations. The method has also the option of designing body shapes by Granville's transition criterion alone.

A number of geometric and aerodynamic constraints are imposed on the design parameters to generate practical and realistic body shapes for given design conditions. The necessary geometric constraints are as follows.

$$r_{Lf_i} < r_{f_i} < r_{Uf_i}; \qquad (i=1,..n_f) \qquad (1)$$

$$r_{La_i} < r_{a_i} < r_{Ua_i}; \qquad (i=1,..n_a) \qquad (2)$$

Judicious choice of the upper and the lower bounds for the design variables will accelerate convergence of the solutions. The level and the location of the minimum surface pressure along the body surface are aerodynamically constrained by the requirement that the turbulent boundary layer over the aft-portion of the body should not separate until x=0.95 for the design conditions. The minimum length of the pressure recovery section for a given minimum pressure level for an axisymmetric body shape can be described by a modified Stratford model, derived for bodies of revolution by Smith, et al. [22 and 32]. Aerodynamic design constraints in the optimization method can also be imposed to avoid strong shock waves [33].

The objective function is taken to be a function of the location of transition predicted by one of the following transition criteria:

$f_{obj} = 1 - x_{tr}(g)$ if Granville's transition criterion alone is used in the design method,

$f_{obj} = 1 - x_{tr}(e^n)$ if e^n-method transition criterion alone is used in the design method

If the "hybrid" transition criterion is used,

$f_{obj} = 1 - x_{tr}(g)$ for calculating gradients of the objective function,

$f_{obj} = 1 - x_{tr}(h)$ for calculating the objective function from a proposed set of design variables at the end of each iteration,

where $x_{tr}(h) = (x_{tr}(g) + x_{tr}(e^n))/2$,

$x_{tr}(g)$ is the transition location predicted by using Granville's transition criterion and

$x_{tr}(e^n)$ is the transition location predicted by using e^n-method with an n-factor of 9.

(3)

The objective function given by Eqn. (3) is to be minimized subject to the constraints described in Eqns. (1 and 2). The optimizer computes gradients of the objective function using Granville's transition criterion and then, using either a conjugate direction method or a method of feasible direction, determines a linear search direction, along which a new constrained variable is constructed.

An improved or minimum feasible objective functional value is calculated by using the hybrid transition criterion given by Eqn. (3) and a series of proposed updated design variables are calculated. The objective function and the constrained function are evaluated using the updated design variables, interpolating over the range of feasible proposed design variables resulting in a minimum value of the objective function. The results are tested against a convergence criteria. The procedure will stop if the convergence criterion is satisfied, giving a body shape with maximum transition length satisfying the separation constraint. If the convergence criterion is not satisfied the design parameters go through the analyzer again resulting in a new set of design variables and the procedure is repeated until a final body shape is obtained.

DETAILS OF THE DESIGN METHOD

The present computational procedure is used to design axisymmetric bodies at zero incidence. At zero incidence, the growth of the 2-D, T-S disturbances is the most dominant instability mechanism on an axisymmetric body leading to transition in the boundary layer if laminar separation does not happen earlier than natural transition. Crossflow vortex structure can develop on the body at nonzero angles of attack. These crossflow vortices can interact with T-S waves and may lead to premature transition. Such complex three-dimensional boundary-layer flows are the subject of current boundary-layer transition investigations and are not considered here.

The axisymmetric body in the present design method is modelled by a set of body ordinates r_{f_i} $(i=1,n_f)$ and r_{a_i} $(i=1,n_a)$. For the aerodynamic analysis the body is modelled by 32 panels in the axial direction and 8 panels in the circumferential direction. Using the VSAERO panel method inviscid pressure distributions were obtained and interpolated at 200 axial stations. The boundary-layer velocity and temperature profiles are obtained with 101 points in the direction normal to the surface and 90 stations in the streamwise direction. The boundary layer calculations are carried out for adiabatic wall conditions and zero suction through the wall.

The boundary-layer stability equations for the example considered are solved at every 5^{th} streamwise boundary-layer station starting from the first station though it is possible to perform the boundary-layer stability calculations at every axial boundary-layer station. The boundary-layer stations are skipped from the point of view of reducing the computational time and it has been observed that this reduction in the number of boundary-layer stations for stability calculations does not change the overall results and the conclusions drawn in this investigation. In the global search for eigen values, the sixth-order stability equation obtained by neglecting dissipation terms in the boundary-layer stability equations, is solved at each chordwise station and the

full eighth order stability equation is solved to search the eigen values locally. The obliqueness of the T-S waves with respect to the streamlines (ψ) in pure axisymmetric flow does not occur until the local flow speed exceeds the local sonic speed. The current version of the program allows the user to specify the wavelength, wave angle, (ψ) and frequencies of the T-S disturbances in subsonic laminar-boundary layer flow. Prior knowledge of the critical boundary-layer disturbance frequencies, which are functions of the Mach number helps to identify the critical frequency spectrum during the course of the design optimization. The present formulation of the stability equation does not include transverse-curvature effects and the effect of streamline divergence (i.e., T-S wave stretching in the nose region-generally termed as vortex stretching, [34]). In general, transverse surface curvature has a slightly stabilizing influence on T-S disturbance growth if the curvature is large in relation to the thickness of the boundary layer [35]. Vortex stretching effects are considerably less if the body has a very small nose radius. If the design constraints are such that a body with a large nose radius is desired, the vortex stretching effects have to be included in the boundary layer stability analysis. The present design calculations do not take into account the effect of the vortex stretching. During the course of the design calculations concave curvature may develop on the axisymmetric body. It is known that centrifugal instabilities in the form of Gortler vortices occur in the shear flow over concave surfaces [36, 37]. In the present design method the boundary layer stability calculations do not consider the effect of the centrifugal instabilities.

To assess the effect of extending the length of laminar boundary-layer flow over the geometries analysed, calculation of the viscous drag is made using a modified integral boundary layer approach [3]. An improved turbulent boundary-layer calculation method is incorporated in the aerodynemic panel method to predict drag coefficients. The turbulent boundary-layer calculations are based on Head's entrainment method as modified by Shanebrook and Sumner [38]. Validation of this improved method with experimental drag measurements by Gertler [39] on axisymmetric turbulent body shapes at R_L of 10.0×10^6 and 26.0×10^6 shows that the drag coefficient can be calculated accurately for the predominantly turbulent flow geometries considered in [3].

COMPUTATIONAL RESULTS AND DISCUSSIONS

To increase the speed of computations the design program is run with the initial body geometry using Granville's transition criterion to obtain a converged body shape. The final body shape obtained by using Granville's criterion is then used as the initial geometry input into the design program and the hybrid transition criterion is selected. This procedure greatly reduces computer time and also results in rapid convergence of the design variables.

Results obtained by the optimization procedure are discussed through an example. All the computations were done on a CRAY-2 computer. A body of revolution whose maximum diameter and length correspond to those of a tiptank of a representative business aircraft is considered. The tiptank has a fineness ratio of 8.00 and the design flight conditions considered for the present calculations are given by M=0.7 and $R'=1.28\times10^6$/foot. The axisymmetric body is modelled by a set of 27 body coordinates with 12 points defining the forebody section (n_f=12) and 15 points defining the aftbody section (n_a=15). Figure 3 presents the pressure distribution on the baseline tiptank and the results of the compressible linear stability analysis for several T-S disturbance frequencies. The pressure coefficients remain subcritical on the entire body. The figure shows that the most critical disturbance reaching an n-factor of 9 has a frequency in the neighborhood of 3500 Hz. Transition onset is predicted to occur for this tiptank shape at $x_{tr}(e^n) = 0.33$ ($R_{tr}(e^n) = 6.04\times10^6$).

For this initial body, transition is predicted by Granville's criterion at $x_{tr}(g) = 0.14$ corresponding to a transition Reynolds number ($R_{tr}(g) = 2.55\times10^6$). As noted in [3], the Granville's transition criterion clearly underpredicts the onset of transition for this body compared to the e^n-method with n=9. The design program with Granville's transition criterion is run with the original tiptank geometry as input. The improvements in the transition locations as the iterations progress are presented in Table 1. Twelve design variables representing the ordinates in the forebody region are allowed to vary within the set of specified upper and lower bounds while simultaneously holding the tail section aft of the maximum thickness point unchanged during the design iterations. Table 1 shows that convergence in the transition location is obtained after 10 iterations. From the table it is also evident that as the number of iterations increase the transition location as computed by Granville's transition criterion shifts downstream. The transition is predicted at $x_{tr}(g) = 0.32$ ($R_{tr}(g) = 5.86\times10^6$) for the final body shape designed by Granville's transition criterion. The transition locations predicted by Granville's criterion for the original tiptank and the final body shape are shown in Fig. 4. The drag coefficients for each iteration, calculated with frontal area as the reference area (Area based on the volume of the body ($V^{2/3}$) is generally used as a reference area for minimizing drag of airships, submarines, cargo-carrying aircraft fuselages etc.) are also presented in the Table 1. The computational time taken was 335 secs.

The final body shape obtained at the end of the optimization with Granville's criterion is used as input to the design program with the hybrid transition criterion. In the present example, since the axisymmteric flow is subcritical, ψ=0 deg is assumed in the design calculations. In general, the spectrum of T-S disturbance frequencies should be chosen such that it does not exclude any disturbance frequencies which may grow substantially on a new body shape generated during the design iterations. In the present example, the body shapes do not go through large perturbations as the number of iterations increases; and, hence, the initially chosen set of T-S frequencies contains all the growing disturbances throughout the design calculations. The same set of T-S disturbance frequencies which is used in the linear stability analysis for the original tiptank is used in the design optimization.

The original tiptank and the final body shape obtained at the end of the ninth iteration using the hybrid transition criterion along with the results of stability analyses are shown in Fig. 5 for comparison. The envelope for the new body shape has a smaller gradient than on the original tiptank shape. On the original tiptank, high frequency disturbances (5000 Hz, 6000 Hz and 7500 Hz) grow up to about 20% of the body length from the nose and then become stable. These high frequency disturbances do not grow beyond an n-factor of 5. The critical disturbance, characterized by a frequency of 3500 Hz, starts growing after 13% of the body length from the nose and reaches an n-factor of 9 at $x_{tr}(e^n) = 0.33$ ($R_{tr}(e^n) = 6.04\times 10^6$). A drag coefficient ($C_D$) of 0.0491 is predicted on the original tiptank with the boundary-layer transition fixed at x_{tr}=0.33. The design program took 2785 secs. to predict the final design shape with the hybrid transition criterion.

On the designed body the disturbances with frequencies of 3500 Hz and 4000 Hz do not grow as much as they grow on the original tiptank. The disturbance frequency of 9000 Hz, which does not grow at all on the original tiptank grows on the new body until an n-factor of about 6 is reached. The disturbance with a frequency of 2500 Hz does not grow at all on the designed body shape and the disturbance with the same frequency grows to an n-factor of about 13 in the case of the original tiptank. The transition location corresponding to n-factor of 9 occurs at $x_{tr}(e^n) = 0.39$ ($R_{tr} = 7.22\times 10^6$) on the designed body. Though the critical frequency leading to transition remains at 3500 Hz on the original tiptank and the designed body, boundary-layer transition as predicted by the e^n-method occurs much further downstream on the designed body. A drag coefficient (C_D) of 0.0415 is predicted on the designed body shape with the boundary-layer transition fixed at x_{tr}=0.39

Volume is not held constant during the design iterations in this example. The original tiptank has a volume of 26.96 cu ft and a surface area of 66.28 sq ft. The total volume and the surface area on the designed body are reduced to 18.13 cu ft and 51.88 sq ft respectively. Most of the volume is lost around the nose portion of the forebody during the optimization. The loss in volume can be made up by redesigning the aft portion of the designed body shape. In future design calculations a volume constraint will also be imposed along with the existing geometric constraints given by equations (1) and (2). The volume constraint along with the geometric constraints will help to design fuselage shapes for aircraft vehicles such as cargo aircraft and airships. Constraints on planform area distribution will be beneficial to optimize the fuselage shape of a passenger aircraft.

The designed body shape has a very small nose radius. Nose shapes with extremely small nose radii will produce large pressure peaks at off-design angles of attack and can produce vortices which would influence transition in a negative way. A constraint on the nose radius will help alleviate the off-design aerodynamic characteristics.

CONCLUDING REMARKS

An optimization procedure has been developed to design axisymmetric body shapes with increased transition Reynolds number. The new design method involves a constraint minimization procedure coupled with analysis of the inviscid and viscous flow regions, and linear stability analysis of the compressible boundary-layer. Boundary-layer transition prediction is predicted by a "hybrid" transition criterion based on Granville's transition criterion and a criterion based on linear stability theory combined with the e^n-method. The method can also be used to design axisymmetric bodies by applying Granville's transition criterion or the criterion based on linear stability method with the e^n-method alone. Since it is found that the design method with the transition criterion based on the e^n-method alone requires large computer resources, the hybrid transition criterion in the design method is more practical. In the hybrid transition scheme Granville's transition criterion is used to compute all the gradients required by the constrained minimization method. At the end of each iteration, an average value of the locations of transition predicted by Granville's transition criterion and the e^n-method transition criterion is then calculated and used in evaluating the objective function. The method can be used to design bodies for specific n-factors to suit a particular flow application.

A tiptank of a business-jet is given as an example to demonstrate that the method can be used to design an axisymmetric body shape with increased transition Reynolds number. Boundary-layer transition is predicted to occur at a transition Reynolds number of 6.04×10^6 on the original tiptank. On the designed body shape a transition Reynolds number of 7.22×10^6 is predicted using the e^n-method, an increase of 20% in transition Reynolds number.

Acknowledgments

The research was supported by NASA Langley Research Center under contract NAS1-18585 to ViGYAN Inc., Hampton.

REFERENCES

[1] Holmes, B.J., Obara, C.J., and, Yip, L, "Natural Laminar Flow Experiments on Modern Airplane Surfaces," NASA TP-2256, June 1984.

[2]. Dodbele, S.S., Van Dam, C.P., and Vijgen, P.M.H.W., "Design of Fuselage Shapes for Natural Laminar Flow," NASA CR-3970, March 1986.

[3] Dodbele, S.S., Van Dam, C.P., and Vijgen, P.M.H.W., Holmes, B.J., "Shaping of Airplane Fuselages for Minimum Drag," Journal of Aircraft, Vol. 24, May 1987, pp. 298-304.

[4] Carmichael, B.H., "Underwater Vehicle Drag Reduction through Choice of Shape," AIAA paper no. 66-657, 1966.

[5] Carmichael, B.H., "Computer Study to Establish the Lower Limit of Length-to-

Diameter Rates Advisable for Low Drag Bodies," SID64-1938, North American Aviation, Inc., 1964

[6] Carmichael, B.H., "Underwater Drag Reduction Through Optimal Shape," In Underwater Missile Propulsion, edited by L. Greiner, Compass Publications, Inc., Arlington, VA 1966.

[7] Vijgen, P.M.H.W., Dodbele, S.S., Holmes, B.J., Van Dam, C.P., "Effects of Compressibility on Design of Subsonic Fuselages for Natural Laminar Flow," Journal of Aircraft, Vol. 25, Sept. 1988, pp. 776-782.

[8] Smith, A.M.O., "Transition, Pressure Gradient and Stability Theory." IX International Congress for Applied Mechanics, Brussels, 1956.

[9] Van Ingen, J.L., " A Suggested Semi-Empirical Method for the Calculation of the Boundary Layer Transition Region," University of Technology, Department of Aerospace Engineering, VTH-74, Delft, 1956.

[10] Hefner, J.N., and Bushnell, D.M., "Status of Linear Boundary-Layer Stability Theory and the e^n-method, with Emphasis on Swept-Wing Applications," NASA TP-1645, Feb. 1980.

[11] Jaffe, N.A., Okamura, T.T., and Smith, A.M.O., "Determination of Spatial Amplification Factors and their Application to Predicting Transition," AIAA Journal, Vol. 8, No. 2, 1970, pp. 301-308.

[12] Bushnell, D.M., Malik, M.R., and Harvey, W.D., "Transition Prediction in External Flows via Linear Stability Theory," IUTAM Symposium Transonicum III, Gottingen, West Germany, May 24-27, 1988.

[13] Malik, M.R. "Instability and Transition in Supersonic Boundary Layers," Laminar Turbulent Boundary Layers (Eds: E.M.Uram and H.E. Weber), Energy Resources Technology Conference, New Orleans, Louisiana, Feb 12-16, 1984.

[14] Dodbele, S.S., "Effects of the Forebody Geometry on Subsonic Laminar Boundary Layer Stability," in Numerical Methods in Laminar and Turbulent Flows,", Pineridge press, Vol.5, Part 1, pp. 902-917, 1987.

[15] Boltz, E.W., Kenyon, G.C., and Allen, C.Q., "The Boundary-Layer Transition Characteristics of Two Bodies of Revolution, a Flat Plate, and an Unswept Wing in a Low-Turbulence Wind Tunnel," NASA TN D-309, April 1960.

[16] Boltz, E.W., Kenyon, G.C., and Allen, C.Q., "Measurements of Boundary-Layer Transition at Low Speeds on Two Bodies of Revolution in a Low-Turbulence Wind Tunnel," NACA Research Memorandum, RM A56G17, Sept 1956.

[17] Vijgen, P.M.H.W., Dodbele, S.S., Pfenninger, W., Holmes, B.J., "Analysis of Wind-Tunnel Boundary-Layer Transition Experiments on Axisymmetric Bodies at Transonic Speeds Using Compressible Boundary Layer Stability Theory," AIAA paper no. 88-0008, 1988, to appear in AIAA Journal.

[18] Dalton, C., and Zedan, M.F., "Design of Low Drag Axisymmetric Shapes by the Inverse Method," Journal of Hydronautics, Vol. 15, Jan.-Dec 1981, pp. 48-54.

[19] Parsons, J.S., Goodson, R.E., and Goldschmied, R.F. "Shaping of Axisymmetric Bodies for Minimum Drag in Incompressible Flow," Journal of Hydronautics, Vol. 8, No. 3, July 1974, pp. 100-107.

[20] Pinebrook, W.E., and Dalton, C. "Drag Minimization on a Body of Revolution Through Evolution," Computer Methods in Applied Mechanics and Engineering, Vol 39, 1983, pp. 179-197.

[21] Wolfe, W.P., and Oberkampf, W.L., "A Design Method for the Flow Field and Drag of Bodies of Revolution in Incompressible Flow," AIAA paper 82-1359, Aug 1982.

[22] Smith, A.M.O. Stokes, T.R., Lee, R.S., "Optimum Tail Shapes for Bodies of Revolution," Journal of Hydronautics, Vol. 15, Nos 1-4, Jan- Dec 1981, pp. 67-73.

[23] Vanderplaats, G. N, "CONMIN - A Fortran Program for Constrained Function Minimization," NASA TMX- 62282, 1973.

[24] Gill, P E, Murray, W, "Quasi-Newton Methods for Unconstrained Optimization," J. Inst. Maths. Applics. 9(1972), pp. 91-108.

[25] Rechenberg, I, "Evolutionsstrategie," Frommann- Holzboog Stuttgast-Bad Cannstatt, W. Germany.

[26] McGhee, R J, Viken, J K, Pfenninger, W, Beasly, W D, Harvey W D, "Experimental Results for a Flapped NLF Airfoil with High Lift Drag Ratio," NASA TM- 85788, May 1984.

[27] Maskew, B., "Prediction of Subsonic Aerodynamic Characteristics- A Case for Low Order Panel Methods,"

[28] Green, L.L., and South, J.C., "Conservative Full-Potential Calculations for Axisymmetric Transonic Flows," AIAA Paper 81-1204, June 1981.

[29] Harris, J.E., and Blanchard, D.K., "Computer Program for Solving Laminar, Transitional, or Turbulent Compressible Boundary-Layer Equations for Two-Dimensional and Axisymmetric Flow," NASA TM 83207, Feb 1982.

[30] Malik, M.R., "COSAL- A Black-Box Compressibility Stability Analysis Code for Transition Prediction in Three-Dimensional Boundary Layers," NASA CR 165925, May 1982.

[31] Gaster, M., "Propagation of Linear Wave Packets in Laminar Boundary-Layers," AIAA Journal, Vol. 19, 1981, pp. 419-423.

[32] Smith, A.M.O., "Stratford Turbulent Separation Criterion for Axially Symmetric Flows," Journal of Applied Mathematics and Physics, (ZAMP), Vol 28, 1977, pp 929- 939.

[33] Murman, E M; and Chapman, G T: "Aerodynamic Design Using Numerical Optimization," NASA TM-85550, Feb 1983.

[34] Kuethe, A.M., "On the Stability of Flow in the Boundary-Layer Near the Nose of a Blunt Body," U.S. Air Force Project RAND RM-1972, ASTIA Doc. No. 150687, 1957.

[35] Morris, P.J., and Byon, W., "The Stability of the Axisymmetric Boundary-Layer on a Circular Cylinder," AIAA paper no. 82-1012, 1982.

[36] Floryan, J.M., and Saric, W.S., "Stability of Gortler Vortices in Boundary Layers," AIAA Journal 20 (4), 1982, pp. 316-324

[37] Hall, P., "The Gortler Vortex Instability Mechanism in Three-Dimensional Boundary-Layers," Proc. R Soc. London Ser. A 399, pp.135-152, 1985.

[38] Shanebrook, J.R., and Sumner, W.J., "Entrainment Theory for Axisymmetric, Turbulent Incompressible Boundary Layers," Journal of Hydronautics, Vol. 4, Oct. 1970.

[39] Gertler, M., "Resistance Experiments on a Systematic Series of Streamlined Bodies for Application to the Design of High-Speed Submarines," David Taylor Model Basin Rept, C-297, April 1950.

Table 1. Convergence of the transition location by Granville's criterion and the drag coefficient for the tiptank example.

f_r=8.003, R_L=18.436×10^6, M=0.7

No. of Iterations	x_{tr}	C_D
Initial	.138	.0600
1	.164	.0568
2	.155	.0572
3	.155	.0572
4	.165	.0566
5	.278	.0495
6	.285	.0464
7	.286	.0458
8	.311	.0448
9	.317	.0445
10	.317	.0445

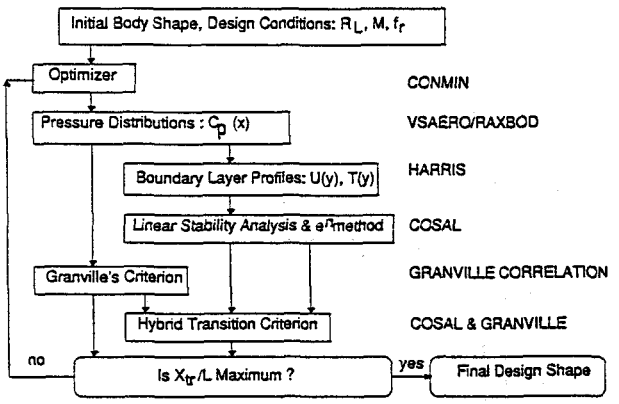

Fig. 1. Flow Chart of design procedure for NLF fuselage

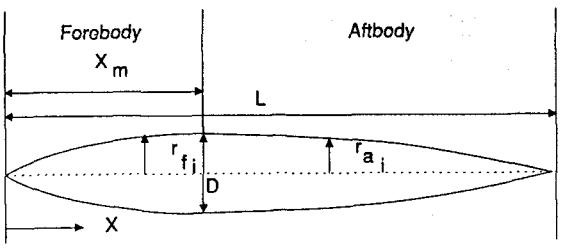

Fig. 2. Definition of design parameters in the optimization procedure.

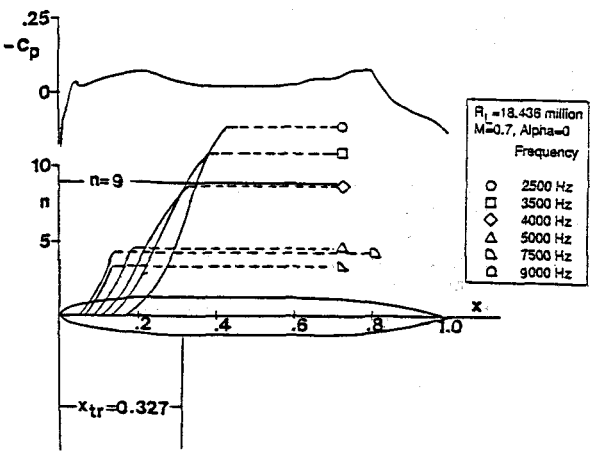

Fig. 3. Pressure distribution and predicted compressible T-S disturbance growth curves and transition on the original tiptank

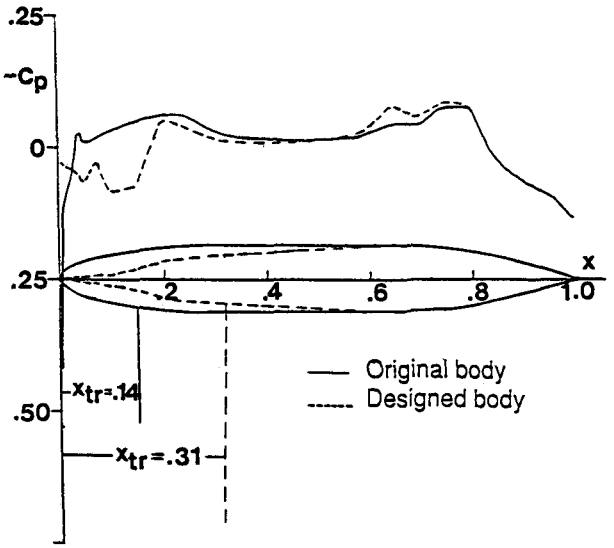

Fig. 4. Pressure distributions, predicted transition locations on the original tiptank and the final design shape (optimization by Granville's transition criterion)

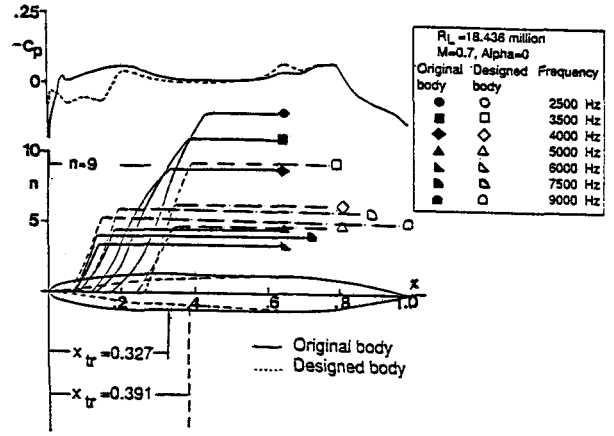

Fig. 5. Pressure distributions, predicted compressible T-S disturbance growth curves and transition locations on the original tiptank and the final design shape (optimization by hybrid transition criterion)